

DRAGON 2-D SIMULATION OF SPATIAL SELF-SHIELDING EFFECT IN SLOWPOKE-2 REACTOR

H. Raouafi, G. Marleau

Institut de génie nucléaire, École Polytechnique de Montréal, Montréal, Canada

Abstract

Thermal and epithermal neutron spatial self-shielding plays an important role in neutron activation experiments, neutron radiography, and reactor physics. Recently, an empirical equation was proposed to calculate the spatial self-shielding factors for neutron activation analysis for some regular geometry. Here, we use the DRAGON code to evaluate these factors for cylindrical samples irradiated in the SLOWPOKE-2 reactor. The DRAGON based self-shielding factors are then compared with the proposed empirical equation and corrections are proposed to increase the reliability of these equations.

1. Introduction

The SLOWPOKE-2 reactor at École Polytechnique de Montréal is mainly used for neutron activation analysis (NAA). The NAA technique is based on the fact that the irradiation of an unknown sample with a neutron flux leads to capture reactions thereby producing radioactive isotopes that decay by γ emission. After irradiation in the reactor, the γ emission spectrum of the sample is counted from which the initial isotopic composition of the sample can be inferred. This method of analysis generally provides a very accurate means to determine the chemical composition of the sample. However, for samples with a high concentration of strong neutron absorbing elements, the NAA results must be corrected since they lead to an under-prediction of the isotopic concentration because fewer neutrons are able to travel long distances in the sample. This effect is known as spatial self-shielding of the sample.

Empirical formula have been proposed to compute thermal and epithermal self-shielding factors for different geometry [1, 2]. These factors depend on the isotopic contents and the dimensions of the sample as well as the flux spectra in the reactor. One alternative to relying on these empirical relations is to evaluate directly the self-shielding effect using the neutron flux distribution inside the sample computed with a neutron transport code. Here we will use the lattice code DRAGON to perform such calculations [3].

In Section 2 of the paper we present the theory of spatial self-shielding for NAA while in Section 3 we discuss the methodology used for the DRAGON simulations. The results we obtained using DRAGON are presented in Section 4 and compared with the empirical self-shielding factors presented in the literature. Finally, in Section 5 we conclude.

2. Theory

The goal of NAA is to produce by neutron irradiation a radioisotope that can be identified accurately from its γ emission spectrum [4]. In fact, following a neutron capture by nuclide A_ZX , a new nuclide $^{A+1}_ZX^*$ is formed in an excited state before it decays according to:



The activity of nuclide $^{A+1}_ZX^*$ is usually expressed as the sum of the contributions from thermal and epithermal neutrons [5]:

$$A = N(G_{th}\sigma_{th}\varphi_{th} + G_{ep}\sigma_{ep}\varphi_{ep})(1 - e^{-\lambda t_i}) \quad (2)$$

where N is the number of atoms of the target nuclide, σ_{th} and σ_{ep} are the thermal and epithermal neutron activation cross sections and, φ_{th} and φ_{ep} are the unperturbed thermal and epithermal fluxes averaged over the volumes of the infinite diluted sample. In Eq. 2, the terms G_{th} and G_{ep} are the thermal and epithermal neutron self-shielding factors. In their papers, I.F Gonçalves *et all* [1, 2] provide a general definition of these factors for cylinders of radius R and height h . They are defined as the ratio between the radiative capture rates per atom in the sample and that in a similar and infinitely diluted sample. Thus:

$$G(R, h) = \frac{\int_{E_1}^{E_2} \varphi(E)\sigma_{n\gamma}(E)dE}{\int_{E_1}^{E_2} \varphi_0(E)\sigma_{n\gamma}(E)dE} \quad (3)$$

Here, $\varphi(E)$ and $\varphi_0(E)$ are respectively the average flux per unit energy inside the real sample and inside infinitely diluted sample, $\sigma_{n\gamma}(E)$ is the (n, γ) cross section and E_1 and E_2 are the lower and the upper limits of the energy region considered. Following the works of Blaauw [6], the thermal self-shielding of neutrons is a function of the total macroscopic cross section Σ_t and macroscopic absorption cross section Σ_a of the sample. Gonçalves *et all* have showed that G_{th} can be represented by sigmoid function for cylindrical sample:

$$G_{th} = \frac{1.00}{1 + (z/z_0)^{1.061}} \quad (4)$$

where $z_0=0.635$ and z is an empirical parameter, deduced from a global analysis of various experimental studies. The proposed formula for this parameter is:

$$z = \frac{Rh}{(R+h)} \Sigma_t \left(\frac{\Sigma_a}{\Sigma_t} \right)^k \quad (5)$$

with $k = 0.85 \pm 0.05$.

For the epithermal self-shielding factor, one must use instead:

$$G_{ep} = \frac{0.94}{1 + (z/z_0)^{0.82}} + 0.06 \quad (6)$$

with $z_0 = 0.270$ and z defined as:

$$z = 1.65 \frac{Rh}{(R+h)} \Sigma_t(E_{res}) \left(\frac{\Gamma_\gamma}{\Gamma} \right)^{1/2} \quad (7)$$

Here $\Sigma_t(E_{res})$ is total macroscopic cross section at resonance peak of total and radiative widths Γ and Γ_γ respectively.

Since the aim of NAA is to determine the concentration of elements in a sample, a better parameter to express self-shielding is the mass of element in the sample. To adapt Eqs. 4 and 6 to NAA, Chilian *et al* [5], propose the following form:

$$G_{th} = \frac{1.00}{1 + (m/m_{th})^{0.964}} \quad (8)$$

$$G_{ep} = \frac{0.94}{1 + (m/m_{ep})^{0.82}} + 0.06 \quad (9)$$

Here m_{ep} and m_{th} can be thought of as the masses of the element that cause respectively 50 % epithermal and 50 % thermal self-shielding for a given cylinder size.

3. DRAGON simulation

3.1. Geometry models

In this work we define two models; the first consists in an exact description of the SLOWPOKE-2 reactor, and the second involves a simplified geometry containing a homogenized fuel-moderator mixture.

For the exact model illustrated in Fig. 1, all the mixtures are taken at 40 °C. On the first level of the geometry, seven annular cells are defined including a central water region (without the control rod), the control rod guide site, the coolant region, the beryllium reflector, the water reflector, the calandria, and part of the water in the pool which extends to 35.56 cm [7]. The second level contains the fuel (uranium oxide fuel enriched at 19.76 %) and its sheathing, two small outer irradiation sites, three large outer irradiation sites and five small inner sites [8].

The second model is roughly the same as that used in the first level for the exact geometry with the second level limited to the small inner irradiation site that contains the sample. The only difference between the two geometries is given in Table 1.

For increased precision, the sample in irradiation site 1 was subdivided into 4 radial regions in addition to being divided into two half cylinders in a direction perpendicular to a line that extends from the center of the core to the center of the sample (See Fig. 2).

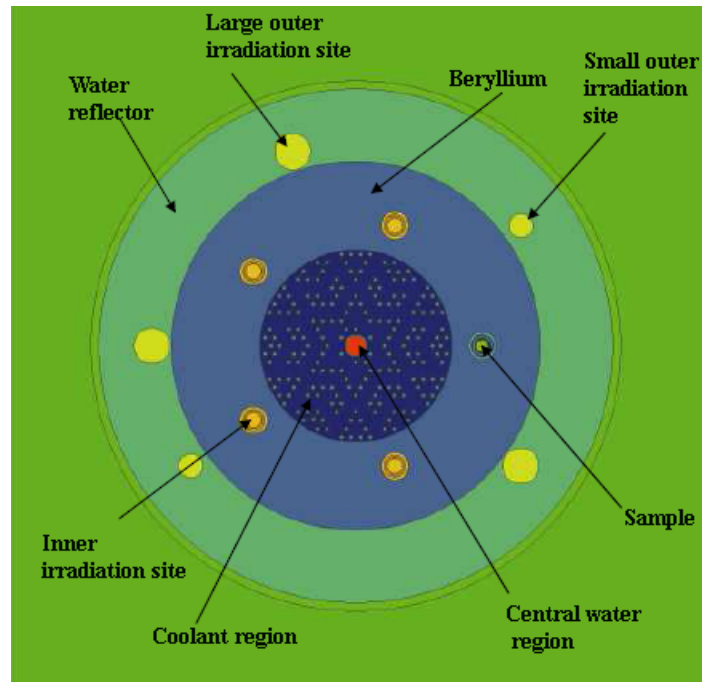


Figure 1: DRAGON exact model for SLOWPOKE-2.

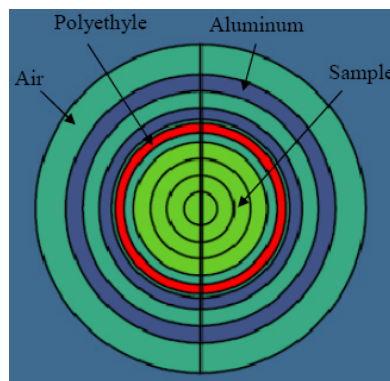


Figure 2: Small inner irradiation site 1 with a sample.

Exact model		Simplified model	
Region name	Mixture number	Region name	New mixture number
Central water region	1	Region 1	1
The control rod guide site	2		
Coolant region	3	Region 2	2
Fuels	4,5,6		
Beryllium	7	Region 3	3
Four small inner irradiation site	8,9		
Water reflector	10	Region 4	4
2 small outer irradiation sites	11		
3 larger outer irradiation sites	11		

Table 1: Mixtures homogenization

3.2. DRAGON sequences of calculation

The sequence of DRAGON modules used for the reference model is illustrated in Figure 3. Here the NXT: module was used to generate tracking information. The collision probability matrices were then built using the ASM: module. The macroscopic cross section library was generated using the LIB: module based on an ENDF/B-VII library with resonance self-shielding calculations performed with the SHI: module. The flux files were then produced by the FLU: module. Homogenization and group condensation were carried out with the EDI: module that produced the final output file.

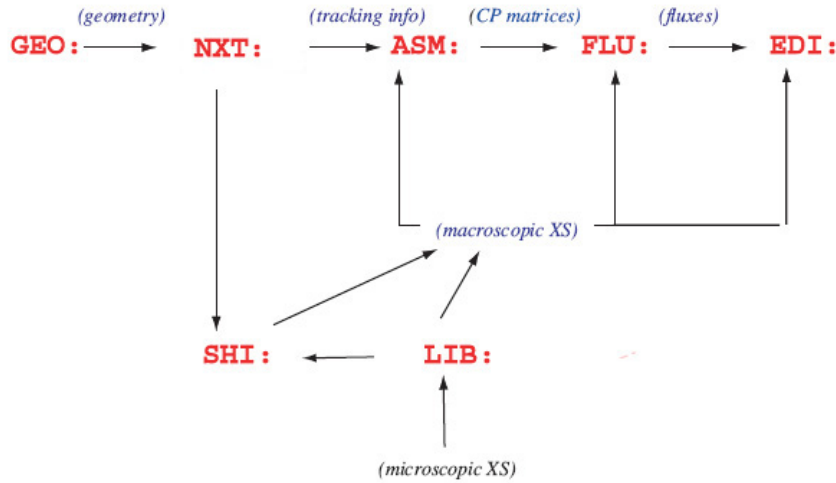


Figure 3: DRAGON calculation sequence

This model runs in 10 hours and 27 minute (Intel Xeon X5650 @ 2.6 GHz). Since one such calculation is required for each type of sample, there is a need to decrease execution time. This is the reason why the simplified model was then introduced.

The calculation procedure for the simplified model is divided into two parts. First, one starts with the exact model and generates, using the EDI: module, region homogenized cross sections (no group condensation is considered here) for the various mixtures required in the model, excluding the irradiation site. Then the general calculation procedure described above is repeated for the simplified model except for the generation of the macroscopic cross section library. Here, the LIB: module is used only to create the macroscopic cross section library associated with the mixtures present in the irradiation site before being combined with the homogenized mixtures obtained from the homogenisation of the exact model.

A second modification to the calculation procedure was also considered. Since our main objective is to evaluate the flux variations in the small irradiation site, the ASM: module was modified in such a way that partial integration of the collision probability (CP) can be considered. To achieve this goal, the MRG: module was first modified so that the tracking file could be subdivided into two parts: 1) a small file that contains all the lines that cross the region of interest (here the irradiation site), and 2) a larger file that contains the remaining lines. Using the second tracking file, ASM: integrates part of the CP associated with regions outside the domain of interest. These can be saved for later use. A second call to ASM: reads the remaining lines and completes the CP integration. In this way, changing the

composition of the material in the irradiation site has no impact on the partial CP and one can restrict the calculation to the final CP integration to the lines in the small tracking file (See Fig. 4).

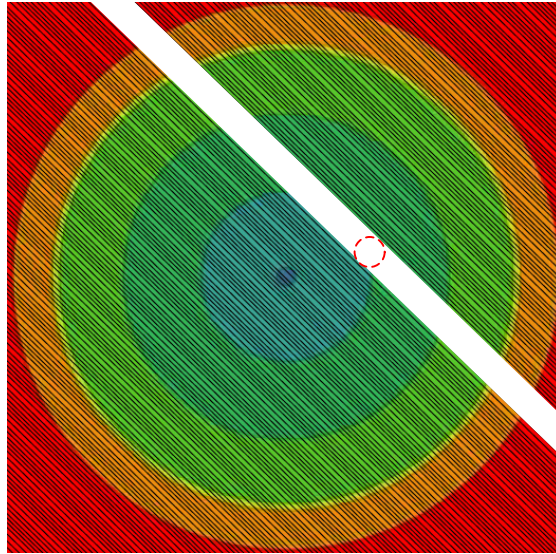


Figure 4: Tracking lines in SLOWPOKE reactor except in small inner site 1

This new calculation procedure proved to be very efficient once the incomplete CP matrix is known (5 minutes of execution for each irradiation site composition compared to more than 10 hours for the reference model).

4. Results and discussion

4.1. Validation of simplified DRAGON model

The exact DRAGON model defined above provides good results for NAA, but with an execution time that is very long. Our aim being to compare simulation results with theoretical expressions, this implies that more than 20 such simulations would be required (10 days of CPU). The second model we propose is much more efficient (10 hours for the first calculation plus an additional 5 minutes per case for a total of 12 hours) and provides an efficient means to evaluate the self-shielding effect of a strongly neutron absorbing sample in an irradiation site.

The thermal and epithermal flux distributions inside a sample presented in Figs. 5 and 6 respectively were obtained for four different cases:

1. Empty sample with exact model (ES/E).
2. Empty sample with simplified model (ES/S).
3. Copper filled sample with exact model (CS/E).
4. Copper filled sample with simplified model (CS/S).

As one can see, both DRAGON models generate very similar thermal and epithermal flux distributions, the thermal flux being slightly larger when the simplified model is considered, leading to a slightly larger epithermal flux. In fact, a reduction in the thermal flux between 0.73% and 1.06% is observed for the simplified model when the copper sample is present while values between 1.33% and 1.60% are

obtained for the empty sample. On the other hand, the epithermal flux for the simplified model increases by 0.32% to 0.93% for the copper sample and between 0.02% and 0.53% for the empty sample.

One can also observe the large flux depression in the thermal flux caused by the presence of the copper sample, this effect being absent in the epithermal flux distribution. This results from the strong thermal absorption cross section of neutrons by copper since neutrons will be mainly captured near the surface leading to a nearly exponential attenuation of the flux towards the center of the sample (See Fig. 5). For the epithermal neutron, slowing down in the reflector is apparent (nearly linear decrease in the flux). Since the epithermal absorption in copper is relatively weak the dip in the curve with the filled sample is much smaller (See Fig. 6).

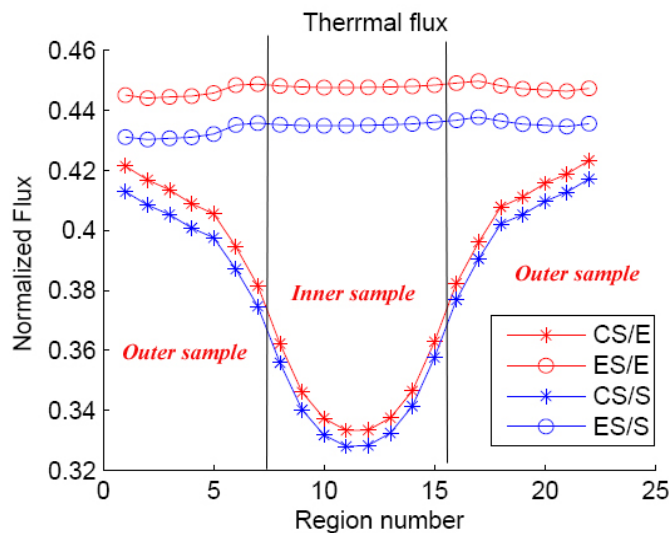


Figure 5: Thermal flux distribution for the exact (in red) and simplified (in blue) models for the empty and copper filled samples.

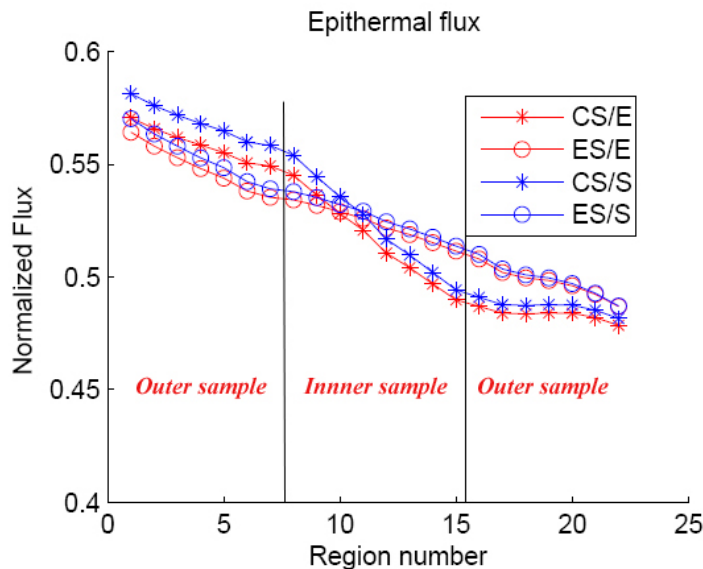


Figure 6: Epithermal flux distribution for the exact (in red) and simplified (in blue) models for the empty and copper filled samples.

4.2. Comparison of DRAGON results with empirical self-shielding relations

Using the above flux distribution, one can now evaluate the spatial self-shielding taking place in a sample using Eq. 3, that for DRAGON can be cast in the form (multi-group and multi-region flux) [10].

$$\frac{\int_{V_i} \int_{E_1}^{E_2} \phi(E, V_i) \sigma_{n\gamma}(E) dE d\vec{r}}{\int_{V_i} \int_{E_1}^{E_2} \phi_0(E, V_i) \sigma_{n\gamma}(E) dE d\vec{r}} \quad (11)$$

This definition is used to calculate self-shielding factors for copper isotope $^{63}_{29}\text{Cu}$ and gold isotope $^{197}_{79}\text{Au}$, where the first isotope is a strong thermal neutron absorber and the second has a large epithermal neutron capture cross section.

Results of our simulations for copper are presented in Fig. 6 and compared with the empirical relations provided in Eq. 8 and 9. One can immediately see that the DRAGON simulations confirm the sigmoid behaviour proposed by Gonçalves [1, 2] to simulate the thermal and epithermal neutron self-shielding effect for copper.

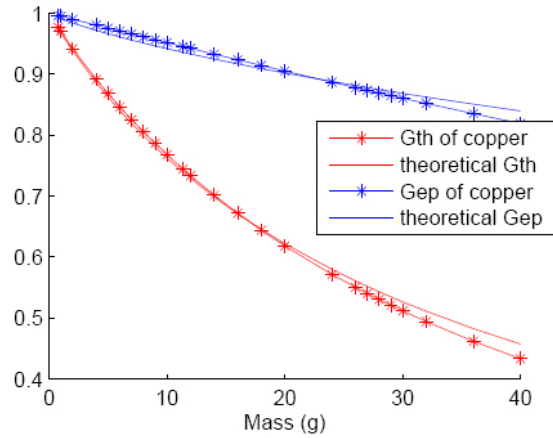


Figure 6: Theoretical versus simulated self-shielding factors for copper

The parameters m_{th} and m_{ep} of both Eqs. 8 and 9 were determined by an iterative procedure using the DRAGON results. Average values of $m_{th}=33.5$ g and $m_{ep}=274.8$ g were obtained. A more appropriate expression for the thermal self-shielding based on our DRAGON simulations would be:

$$G_{th}(m) = \frac{1}{1 + (m/m_{th2})^2 + (m/m_{th1})} \quad (12)$$

with $m_{th1} = 34.8$ g and $m_{th2} = 103.1$ g.

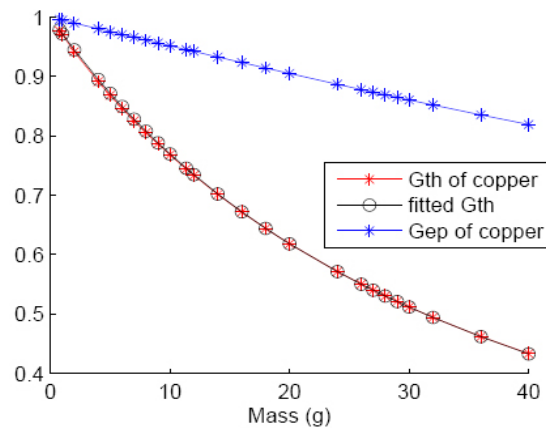


Figure 7: Improved fit for thermal neutron self-shielding factor in copper

In order to confirm this equation, gold was also simulated for the same irradiation site and with the same geometry. First a comparison with Gonçalves' equations confirms again that DRAGON can simulate correctly the epithermal self-shielding effect (See Fig. 8). The parameter m_{th} and m_{ep} were again determined using an iterative procedure, leading to averaged values of 4.1 g and 0.217 g respectively.

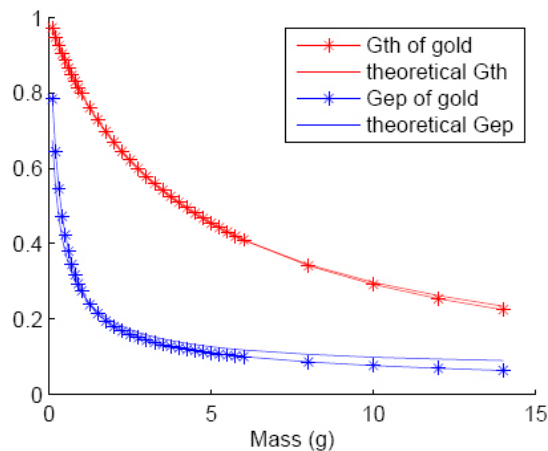


Figure 8: Theoretical versus simulated self-shielding factors for gold

Moreover, using Eq. 12 to simulate the thermal self-shielding factor computed using DRAGON led to a better fit (Fig. 9) with the values for $m_{th1} = 4.35$ g and $m_{th2} = 33.15$ g. Eq. 12 can then be used to correct the empirical equations of Gonçalves.

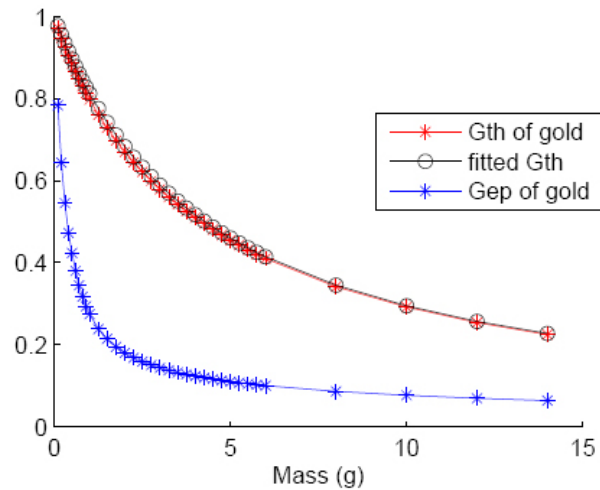


Figure 9: Improved fit for thermal neutron self-shielding factor in gold.

5. Conclusion

The simplified DRAGON 2-D model developed in this work for the SLOWPOKE-2 reactor is very efficient in CPU time and can be used to evaluate both the thermal and epithermal spatial self-shielding factors for samples containing strong neutron absorbers. Using our simulation, we were also able to propose an updated empirical expression to evaluate the self-shielding factors.

Since the goal of NAA is to determine the amount of neutron absorbing isotopes in unknown samples based on measurement, we next plan to program inside a DRAGON input file an iterative procedure that would automatically correct the measured activities when a strongly absorbing isotope is present in the sample.

6. Acknowledgments

This work was supported in part by University Mission of Tunisia in North America (MUTAN), a scholarship from the ROASTERS foundation and the Natural Science and Engineering Research Council (NSERC).

7. References

- [1] I. Gonçalves, E. Martinho, and J. Salgado, "Extension to cylindrical samples of the universal curve of resonance neutron self-shielding factors," *Nuclear Instruments and Methods in Physics Research Section B: Beam Interactions with Materials and Atoms*, vol. 213, pp. 186-188, 2004.
- [2] E. Martinho, J. Salgado, and I. Gonçalves, "Universal curve of the thermal neutron self-shielding factor in foils, wires, spheres and cylinders," *Journal of radioanalytical and nuclear chemistry*, vol. 261, pp. 637-643, 2004.
- [3] G. Marleau, A. Hébert, and R. Roy, "*A User's Guide for DRAGON*," IGE-174, Rev 10, École polytechnique de Montréal, 2012.
- [4] G. REVEL, *Analyse par activation*, Ed. Techniques Ingénieur, 1999.
- [5] C. Chilian, M. Kassakov, J. St-Pierre, and G. Kennedy, "Extending NAA to materials with high concentrations of neutron absorbing elements," *Journal of radioanalytical and nuclear chemistry*, vol. 270, pp. 417-423, 2006.
- [6] M. Blaauw, "The derivation and proper use of Stewarts formula for thermal neutron self-shielding in scattering media," *Nuclear science and engineering*, vol. 124, 1996.
- [7] G. Marleau, S. Noceir, R. Roy, and D. Rozon, "DRAGON modelling of the SLOWPOKE-2 reactor at Ecole Polytechnique," in *1997 CNA/CNS Annual Conference*, vol. 1, Toronto, 1997.
- [8] B. M. Townes, J. W. Hilborn, "The SLOWPOKE-2 reactor with low enrichment uranium oxide fuel," in the *Canadian Nuclear Society 1985 Annual conference*: Chalk River, 1985.
- [9] P. Reuss, *Précis de neutronique*, France: EDP Sciences, 2003.
- [10] A. Hébert, *Applied reactor physics*, Canada: Presses International Polytechnique, 2010.